

DETACHED-EDDY SIMULATION OF FLOW PAST A BACKWARD-FACING STEP WITH A HARMONIC ACTUATION

Liang Wang*, Ruyun Hu*, Liying Li*, Song Fu*

*School of Aerospace Engineering, Tsinghua University, Beijing 100084, China

Abstract

This study conducted Detached-Eddy Simulations of the actively controlled flow over a backward-facing step at a step-height Reynolds number of 64000. Results from the DDES (Delayed DES) and IDDES (Improved DDES) variants are compared with experiments in the base-flow case. IDDES shows mild improvement in agreement with the experimental data and some increase in the resolution of high frequencies. The peak amplitude in the frequency spectrum of the unexcited flow can be found at a Strouhal number of 1.08, which is used as the actuation frequency. However, DDES results indicate that the separation bubble length can be slightly reduced by using a harmonic actuation (zero-net-mass flux) through holes positioned at 0.23 step height upstream the step. The ongoing work will be further calculations for the variation of the actuation frequency and intensities.

1 Introduction

Drag reduction and separation control are directly related to more efficient air transportation and less emission of harmful gases into the environment. Harmonic actuation is one of the most widely used flow-control devices. It however introduces additionally unsteadiness into the separated flow, which present an ideal application for hybrid RANS-LES methods.

The first hybrid RANS-LES method, known as Detached-Eddy Simulations (DES) proposed by Spalart et al. in 1997 [1], is to combine the strengths of the RANS scheme near the solid wall boundaries and LES elsewhere. Following

this, the approach was applied to other RANS models, e.g. based on the $k-\omega$ -SST model [2] proposed by Travin et al. [3]. Since then hybrid RANS/LES methods have found an ever increasing interest, which resulted in elimination of some problems found in the early applications of these methods through appropriate improvements, e.g. the Delayed DES (DDES) method [4] and inspired a large variety of methods not restricted to DES-like approaches, but including also other, "seamless" [5] and zonal [6], methods. The ability to capture separated flows with affordable computational cost has prompted their use over a wide range of application areas, especially for flows with massive separation.

However, the so-called "Grey Area" problem arises in DES. It is that part of the flow domain where the transition between RANS and LES takes place and where despite being in LES mode the flow field does not contain enough resolved turbulence as none is provided by the RANS part. Consequently, an overall turbulence deficit arises, as there is neither sufficient modelled turbulence nor sufficient resolved ones due to its slow development in LES mode, which in turn can compromise the whole simulation.

The backward-facing step (BFS) configuration, forming the basis of many real flow situations, was selected as a standard test case by the on-going EU-China project MARS (Manipulation of Reynolds Stress for Separation Control and Drag Reduction). The main task in this project is to explore the flow control mechanism in relation to manipulation of the turbulent Reynolds stresses. Recently, the researchers within this project experimentally studied an oscillating-surface actuation

upstream the flow separation point of BFS, in which it is unfortunately obtained no positive results in the reduction of the separation bubble length due to insufficient actuation intensity applied.

The objective of this paper is to numerically study the active flow control with a harmonic actuation using Delayed DES (DDES) and Improved DDES (IDDES) methods. This work includes a comparison of URANS with DDES and IDDES.

2 Model description and grid generation

The experiment was carried out by Manchester University in the wind tunnel in APL-UniMan [7]. The wind tunnel has a squared cross section of $0.9 \text{ m} \times 0.9 \text{ m}$, and the length of the test section is 5.5 m . The backward-facing step height, h , is 0.065 m . The upstream length before the step is $53.85h$, and the downstream length behind the step is $30.77h$. The expansion ratio (outlet height/inlet height) is about 1.07 . Considering this small expansion ratio, the top wall effect is negligible for the BFS flow. The Reynolds number based on h and the freestream velocity, U_0 , is of 6.4×10^4 .

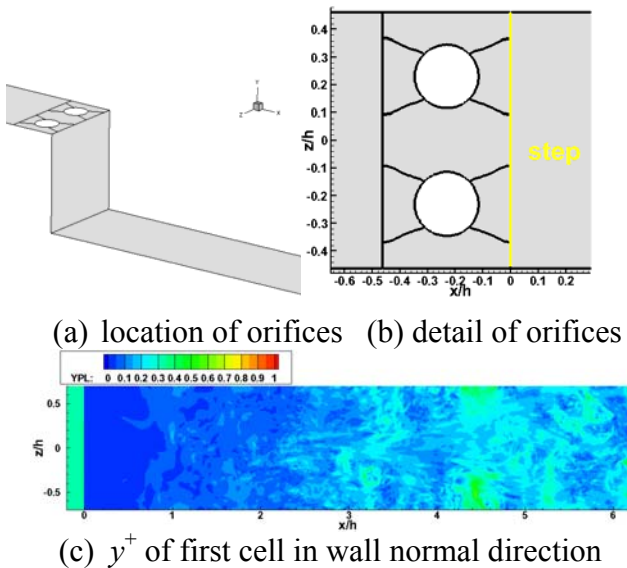


Fig. 1. Backward-facing step and configuration.

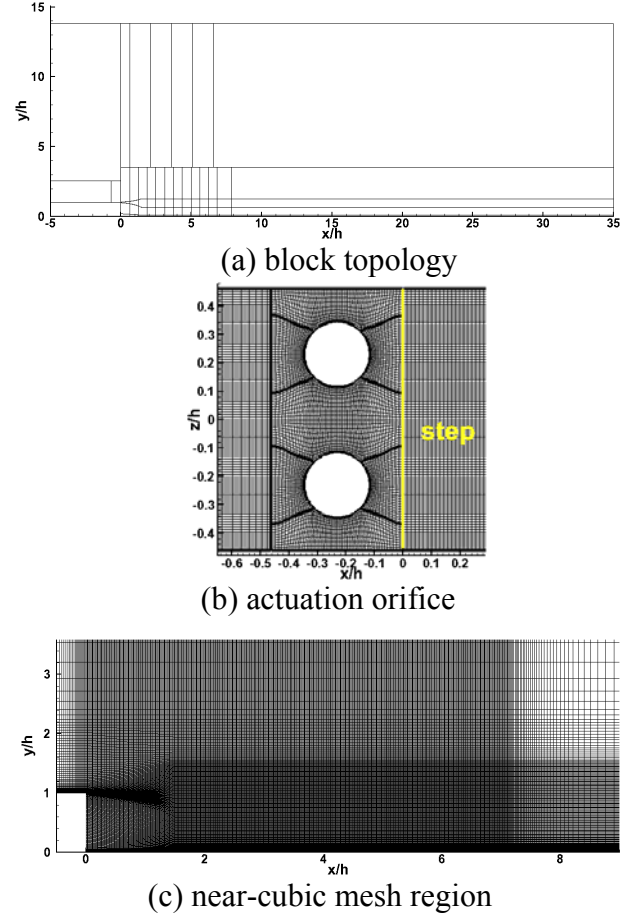


Fig. 2. Topology of the computational mesh.

Incompressible simulations on a computational domain (see Fig. 2a) corresponding to the relatively confined wind tunnel geometry are carried out. At the inlet, $5h$ upstream the separation point, the turbulent boundary-layer thickness equals to h with the Reynolds number based on h , Re_h , of 6.4×10^4 . The upper wall is located $9h$ from the lower wall. The channel outlet is located $35h$ downstream of the step. The domain extends $1.4h$ in the spanwise direction.

The grid system is displayed in Fig. 2. It is designed to provide very fine near-cubic grid cells in the focus region. The grid spacing is no larger than $0.014h$ up to $7h$ downstream of the step.

This grid consists of around 11 million cells and is distributed over 120 CPU cores, whereby an even load balances is achieved. No wall functions are applied and the boundary layers are resolved with at least 45 points in the wall normal direction with y^+ kept below 1 on all elements, as shown in Fig. 1c.

3 Numerical methodology

3.1 In-house flow solver

An implicit pressure-based solver with a fully conservative approximation of the governing equations is employed in the flow simulation. The code is based on curvilinear coordinates and uses cell-centered collocated storage arrangement on semi-block structured grids for all quantities. The two-equation SST- $k-\omega$ model [2] is used here as the underlying model for the DDES [4] and Improved DDES (IDDES) [8] presented here. The C_{DES} parameter is set to 0.52, as calibrated against the decay of isotropic turbulence. In order to best address the inconsistency in the demands posed by RANS and LES on the numerical scheme for the convective fluxes, the blending function of Travin et al. [3] is employed to assure an appropriate switch between a higher-order TVD scheme and central differencing. The diffusive fluxes are approximated using a second order central scheme and for time discretisation second order backward differencing is applied. The continuity equation is conserved by the SIMPLE algorithm whereby the decoupling of pressure and velocity is prevented through a modified Rhie & Chow interpolation. The code is parallelised via domain decomposition and the data interchange between processors is realised through the standardised MPI-library. RANS solutions obtained with the SST model are used as initial condition for the DDES and the IDDES.

3.2 References Improved Delayed Detached Eddy Simulation

The DES method was developed for the simulation of separated flows with the treatment of the entire boundary layer using RANS. This non zonal, hybrid technique was introduced by Spalart et al.[9] in 1997 for the Spalart-Allmaras (SA) turbulence model in order to combine the strengths of RANS and LES. The fundamental advantages of this hybrid approach are manifest both in terms of computational costs and of

accuracy in the prediction of complex wall bounded flows. Furthermore, the high performance of LES in the outer turbulent regions is maintained in the DES technique. The blending is done by modification of the length scale L_{RANS} of the turbulence model. This model length scale is substituted by the DES length scale L_{DES} , which is defined similar to an implicit filter in LES:

$$\begin{aligned}\Delta &= \max(\Delta_x, \Delta_y, \Delta_z) \\ L_{DES} &= \min(l_{RANS}, C_{DES}\Delta)\end{aligned}\quad (1)$$

The method was later generalized to be applicable to any RANS model by Travin et al. [3]. The further investigations on the DES approach showed some problems for critical cases, e.g. Modeled Stress Depletion (MSD) that can lead to Grid Induced Separation (GIS) and the activation of the near wall damping terms of the underlying turbulence model in the LES regions. These problems were addressed by the development of the Delayed Detached Eddy Simulation (DDES) by Menter et al. [10] in 2004 for the SST- $k-\omega$ model and more general in 2006 from Travin et al. [11] in channel simulations with massively refined grids near the walls (LES-like grid) the DES shows two stacked logarithmic layers, which causes a significant and unphysical reduction of the friction coefficient. This effect is called Log Layer Mismatch (LLM). Travin et al. [11] published a method based on the DDES approach in 2006 that has shown promising results for fully-developed turbulent channel flow. This variant is known as ‘‘Improved DDES’’ (IDDES) and has been implemented and validated by the present authors. The major advantage over the former DES variants is the possibility to simulate resolved turbulent boundary layer structures. It will therefore be used for the actual case.

The IDDES approach uses a more complex formulation for evaluating the grid filter Δ and for the blending of the grid filter with the RANS turbulent length scale (L_{RANS}). The grid filter depends additionally on the wall normal distance dw and the height of the cell in wall normal direction h_{wn} :

$$\Delta = \min(\max[C_w d_w, C_w h_{\max}, h_{wn}], h_{\max}) \quad (2)$$

$$h_{\max} = \max(\Delta_x, \Delta_y, \Delta_z)$$

Here C_w is a model constant. The blending is done by the so called ‘‘hybrid function’’, f_{hyb} , that includes the functionality of former developed DDES (f_d) with the shield function Ψ and formulates the modified length scale L_m as follows:

$$L_m = f_{hyb}(1 + f_{restore})L_{RANS} + (1 - f_{hyb})L_{LES} \quad (3)$$

$$\text{with} \quad \begin{aligned} L_{LES} &= C_{DES} \Psi \Delta \\ f_{hyb} &= \max\{(1 - f_d), f_{step}\} \end{aligned} \quad (4)$$

The functions f_d , $f_{restore}$, f_{step} and Ψ are defined in a complex manner by analysis of the local boundary layer flow parameters. The complete description of the IDDES approach is detailed in.

3.3 Numerical setup and parameter

RANS simulations are performed prior to the unsteady simulation using the same turbulence model as used for the DESs. The flow field obtained is used as the initial condition for the unsteady simulation. All the DESs have been run for more than 20 convective time units, $\tau_h = t U_0 / h$, before the evaluation of averages and the storage of the surface data was initiated. The sampling times are at least 30 convective time units for the DESs.

From initial numerical investigations of the configuration without excitation, characteristics of the unsteady behavior are already known. A separate study of the influence of time step size indicated that a typical time step of $\Delta t = 1 \times 10^{-2} h / U_0$ is sufficient to obtain results independent of the temporal resolution. All computations presented here are based on this time step size, e.g. which allows a resolution of around 100 time steps per actuation cycle for the highest non-dimensional actuating frequency of $F^+ = f_{ex} \times h / U_0 = 1.08$.

At the wind tunnel entry all flow quantities including the velocity components and turbulent properties are prescribed. The level of turbulence at the inflow is set to $T_u = (2k/3)^{0.5} / U_0 = 0.5\%$ and the turbulent viscosity $\mu_t / \mu = 0.1$. At the outflow a convective boundary condition is used that allows unsteady flow structures to

be transported outside the domain. The complete airfoil surface is modeled as a non-slip boundary condition. The wind tunnel walls are approximated as inviscid walls.

The ‘‘laminar profile’’ is considered in the present paper. It stands for an actuation boundary condition used to model the velocity profile on a small wall segment. The actuation velocity inlet is placed at its bottom. The time-dependent velocity for the harmonic actuation (see Fig. 3) is modeled as follows:

$$u_{jet}(x, t) = u_a(x) \cdot \sin[2\pi \cdot F^+ \cdot t] \quad (5)$$

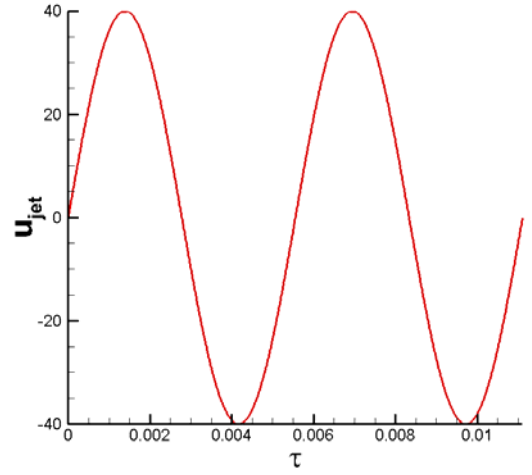


Fig. 3. Modeling of the time-dependent part of the harmonic actuation.

4 Results and discussions

Table 1 lists our three simulations with parameters. The first two cases are incompressible DDES and IDDES for unexcited flow case. The last one employs DDES for the excited flow case. The experimental data [7], our results from the unexcited and excited flow simulations, are labelled as EXP, BASE and EXCITED, respectively.

Table 1. Test case parameters

Case	Model	Structured Mesh	$\Delta t (\times h/U_0)$	Re_h	Sampling time ($\times h/U_0$)
1	SST-DDES	11.3E6	0.01	6.4E4	80
2	SST-IDDES	11.3E6	0.01	6.4E4	40
3	SST-DDES	11.8E6	0.01	6.4E4	80

4.1 DDES vs. IDDES capabilities in base flow case

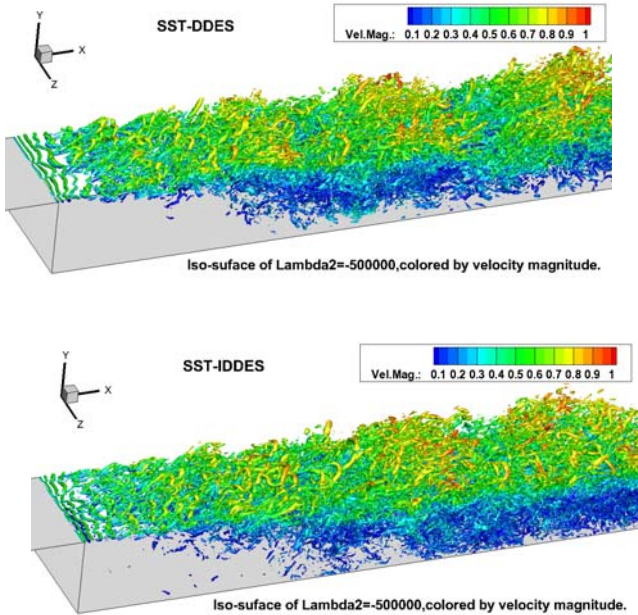


Fig. 4. Instantaneous flow using the λ_2 vortex core criterion at $\lambda_2 = -500000 \text{ s}^{-2}$, shaded by dimensionless velocity magnitude. Results are from DDES (upper) and IDDES (lower), respectively.

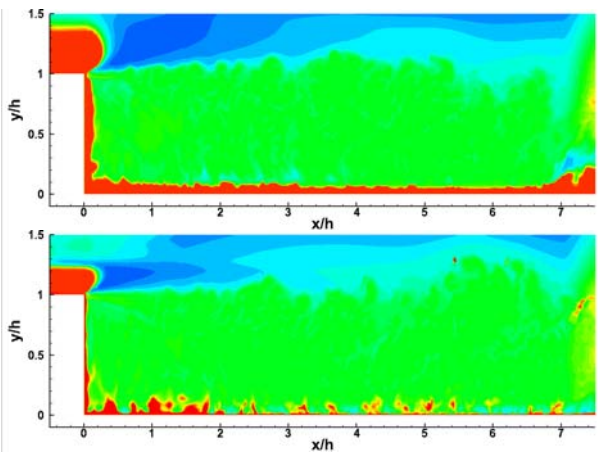


Fig. 5. Comparison of DES functionality for DDES (upper) and IDDES (lower).

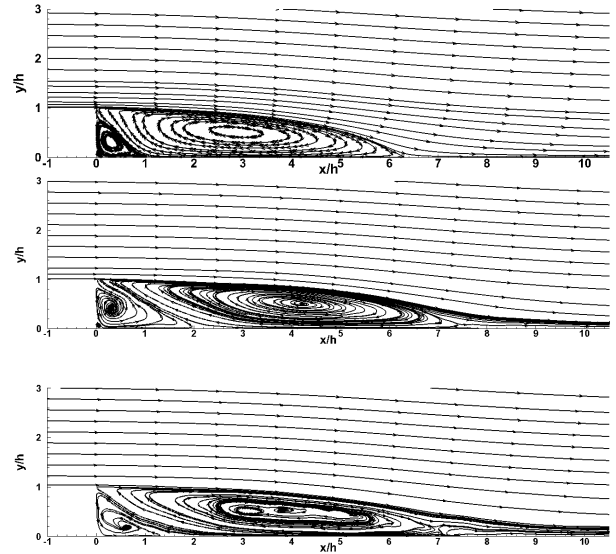


Fig. 6. Streamline pattern downstream of the corner along the mid-span plane, obtained by using URANS (upper), DDES (middle) and IDDES (lower).

Fig. 4 gives a basic description of the flow physics for the unexcited case. The size of the recirculation region and reattachment point is time dependent. Fig. 5 shows the regions in which the alternative modes of DES are in operation, using the ratio of the DES to RANS length scales L/L_{RANS} as an indicator. In this representation a value less than unity corresponds to the LES mode. The much thinner RANS region in IDDES compared to that of DDES is seen.

Fig. 6 further shows averaged streamline pattern near the step along the plane at mid-span. It is seen that downstream the step, a shear layer develops, the flow detaches, and a recirculation region is formed. A small corner eddy exists between the step and the main recirculation zone. The most noticeable difference between DDES and IDDES concerns the prediction of the size of the corner eddy: This remains steady in DDES due to the boundary layer RANS shielding shown in Fig. 5, whereas unsteady fluctuations are resolved by IDDES. The measured reattachment point location, x_{reat} , at $6.5h$ downstream the step is fairly well predicted by URANS, while over-predicted by both DDES and IDDES.

Fig.7 respectively presents the profiles of stream-wise mean velocity U , the R.M.S. of U fluctuations, U_{rms} , and Reynolds shear stress, $\langle uv \rangle$, along the mid-span plane. In attached flows, the mean U profile matches the measured data well, however, all simulations under-predict the turbulent fluctuations; downstream the step, both DDES and IDDES perform much better than URANS. The results of IDDES are on balance slightly closer to experimental data compared to those of DDES.

The dominant amplitude in the frequency spectrum of the global lift coefficient can be found at a Strouhal number of $St = 1.08$ (see Fig. 8a), which correspond to the vortex-shedding characteristics of the unexcited flow. It is used as a starting point for a variation of the actuation frequency F^+ . Fig. 8b indicates that $St = 2.62$ is the characteristic frequency of the shear-layer instability. It should be noted that the smallest frequency (or the St number in the figure) is related to the total time of the sampling (see Table1), and the largest frequency is determined by the sampling frequency, which equals to $1/\Delta t = 100 U_0 / h$. There are some evidences of higher frequencies resolved by IDDES.

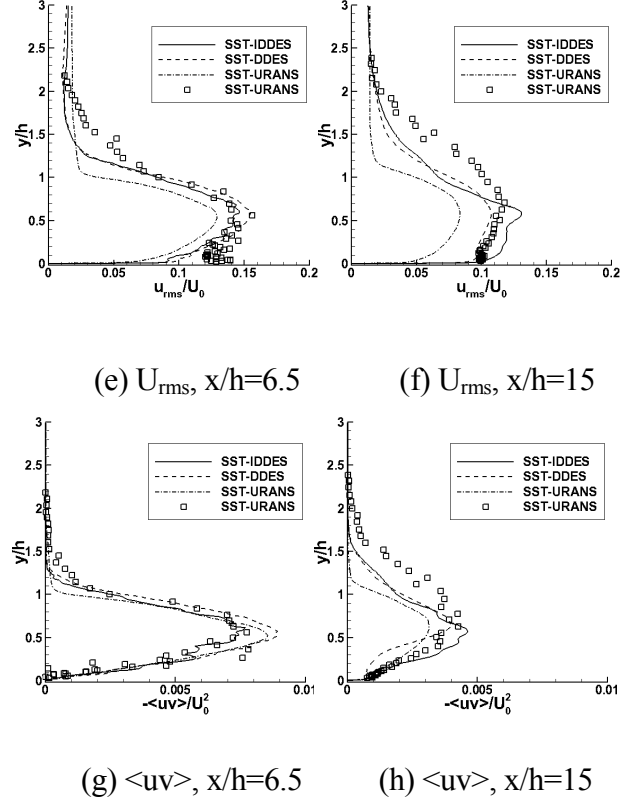
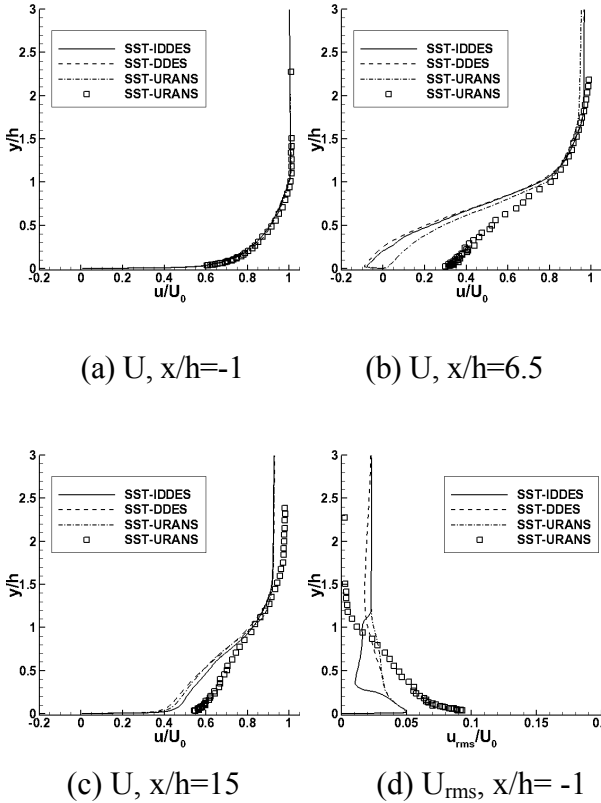
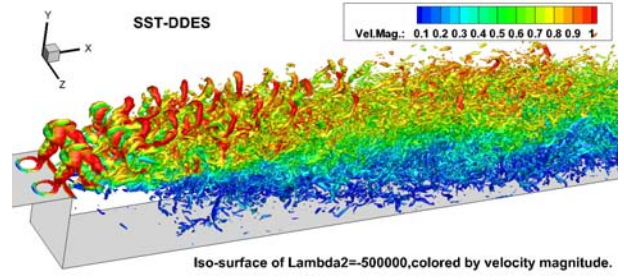
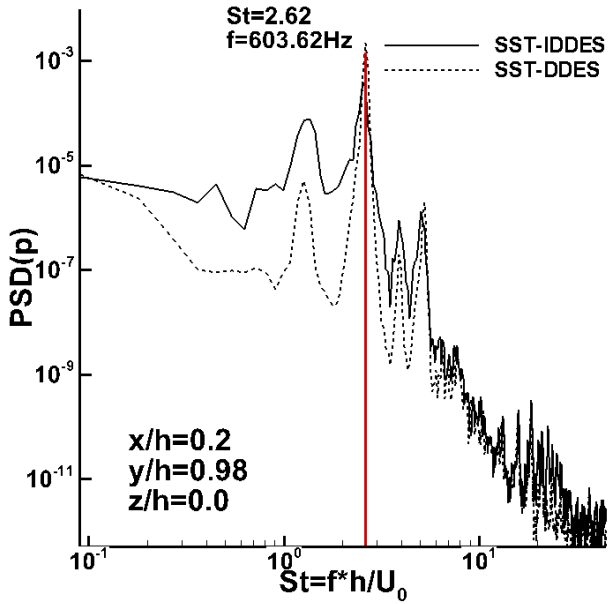
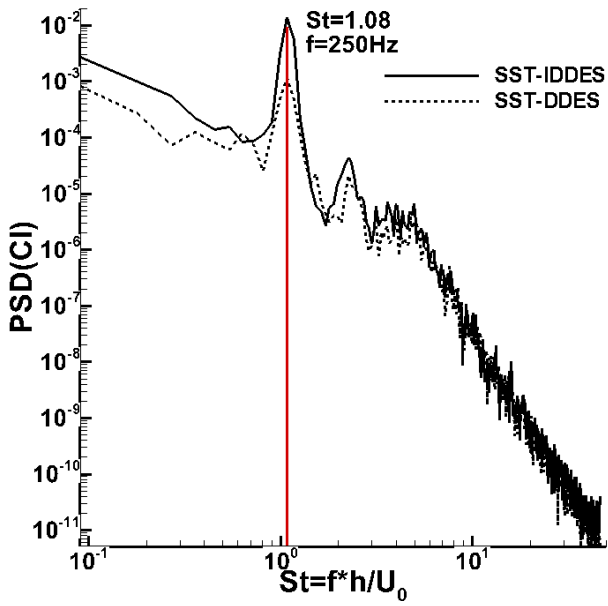


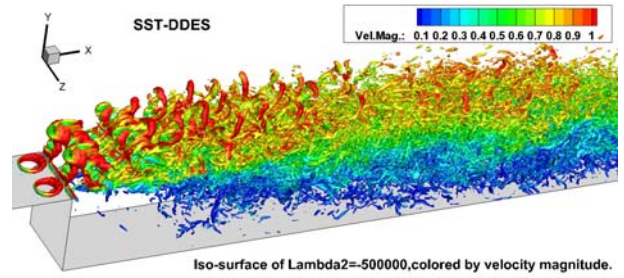
Fig. 7. Calculated and measured profiles of stream-wise mean velocity U , the R.M.S. of U fluctuations, U_{rms} , and Reynolds shear stress, $\langle uv \rangle$, along the mid-span plane.

4.2 Excited flow cases

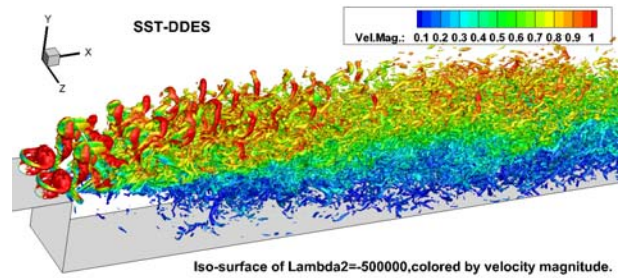
All excited computations use the unexcited case solutions as initial flow conditions. Fig. 9 shows the instantaneous snapshot of the excited flow with harmonic actuation. It is seen that three-dimensional vortex structures are formed at the orifices but however not immersed into the downstream shear layer, under the current actuation conditions, i.e. $F^+ = 1.08$ and $U_{jet} = 200$ m/s. Therefore, the massive separation downstream the step is not suppressed at all, as shown in Fig. 10, which is quantitatively identified by Fig. 11 that the actuation influences the external flow rather than the recirculation region.



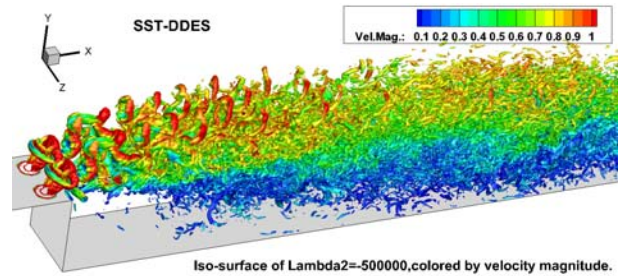
(b) $t = 0.1 T$



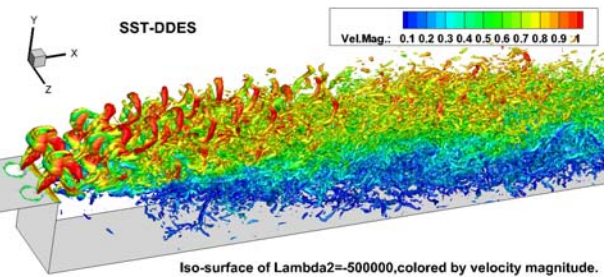
(c) $t = 0.2 T$



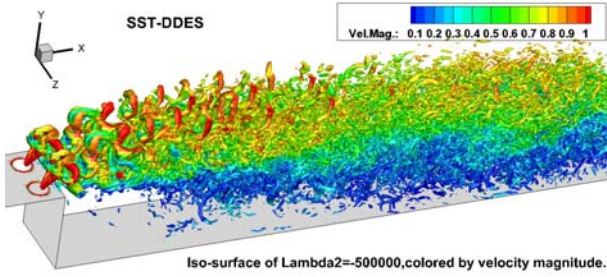
(d) $t = 0.4 T$



(e) $t = 0.6 T$



(a) $t = 0 T$



(f) $t = 0.8 T$

Fig. 9. Instantaneous snapshot (from DDES) of the unexcited flow.

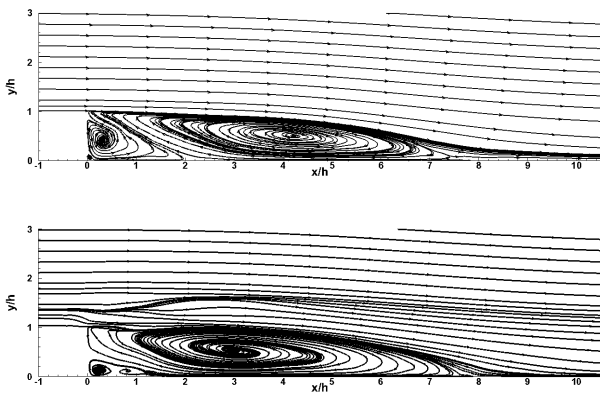


Fig. 10. DDES results of streamline patterns downstream of the corner along the mid-span plane for the unexcited (upper) and the excited (lower) flows.

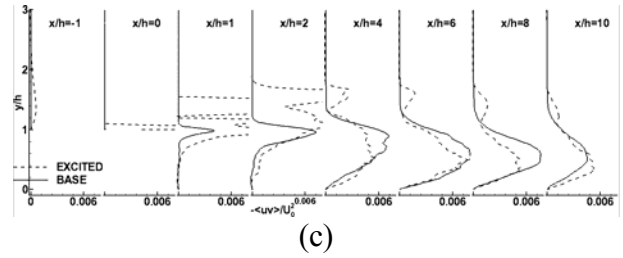
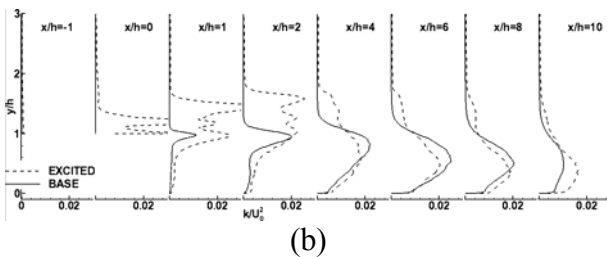
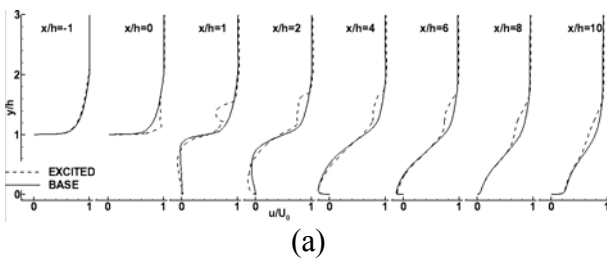


Fig. 11. Calculated profiles of stream-wise mean velocity U (a), dimensionless turbulent kinetic energy, k , and dimensionless Reynolds shear stress (c), $\langle uv \rangle$, along the mid-span plane.

5 Conclusion

In this study, a numerical study of active flow control on a backward-facing step has been conducted. With the use of an in-house finite-volume based flow solver, unsteady Reynolds-averaged Navier-Stokes and detached-eddy simulations have been carried out on a structured grid of 11 million cells, to evaluate the effectiveness of a fluidic excitation mechanism to control the flow separation. The results of IDDES are slightly closer to experimental data compared to those of DDES. The peak amplitude in the frequency spectrum of the unexcited flow can be found at a Strouhal number of 1.08, which is used as the actuation frequency. So far, the harmonic actuation influences the external flow rather than the recirculation region. The ongoing work will be further calculations for the variation of the actuation frequency and intensities.

Acknowledgments

This work is funded by the EU-China project MARS which is jointly supported by EU and MIIT of China. We are also grateful to the National Natural Science Foundation of China for the Grants 10232020, 10932005, 11202115 & 11272183.

References

[1] Spalart P R, Jou W H, Strelets M and Allmaras S R. Comments on the feasibility of LES for wings, and on a hybrid RANS/LES approach. Advances in DNS/LES, Ruston, LA, USA, pp 137-147, 1997.

- [2] Menter F R. Two-equation eddy-viscosity turbulence models for engineering applications. AIAA Journal, Vol. 32, pp 1598-1605, 1994.
- [3] Travin A, Shur M, Strelets M and Spalart P R. Physical and numerical upgrades in the detached-eddy simulation of complex turbulent flows. Proceedings of the Euromech Colloquium 412, Munich, Germany, Vol. 412, pp 239-254,2002.
- [4] Spalart P R, Deck S, Shur M, Squires K D, Strelets M, and Travin A. A new version of detached-eddy simulation, resistant to ambiguous grid densities. Theor. Comput. Fluid Dyn, Vol. 20, pp 181-195,2006.
- [5] Fadai-Ghotbi A, Friess C, Manceau R, and Borée J. A seamless hybrid RANS-LES model based on transport equations for the subgrid stresses and elliptic blending. Physics of Fluids, Vol.22,pp 55-64, 2010.
- [6] Deck S. Zonal-Detached-Eddy simulation of the flow around a high-lift configuration. AIAA Journal, Vol. 43, No. 11 , pp 2372-2384,2005.
- [7] <http://www.cimne.com/cdl1/spacehome/2/0#>
- [8] Shur M, Spalart P R, Strelets M and Travin A. A hybrid RANS-LES approach with delayed-DES and wall-modelled LES capabilities. International Journal of Heat and Fluid Flow, Vol. 29, pp 1638-1649,2008.
- [9] Spalart P R and Allmaras S. A one-equation turbulence model for aerodynamic flows. Proc. 30th AIAA Aerospace Sciences Meeting and Exhibit, Reno, Nevada, USA, pp 1-22,1992.
- [10]Menter F R and Kuntz M. Adaptation of eddy-viscosity turbulence models to unsteady separated flow behind vehicles. The aerodynamics of heavy vehicles: trucks,buses and train, Vol.19, pp 339-352, 2004.
- [11]Travin A K, Shur M L, Spalart P R and Strelets M K. Improvement of Delayed Detached-Eddy Simulation for LES with Wall Modelling. ECCOMAS CFD, Netherlands, 2006.

it as part of their paper. The authors confirm that they give permission, or have obtained permission from the copyright holder of this paper, for the publication and distribution of this paper as part of the ICAS 2014 proceedings or as individual off-prints from the proceedings.

Contact Author Email Address

Prof. Song Fu
mailto: fs-dem@author.com

Copyright Statement

The authors confirm that they, and/or their company or organization, hold copyright on all of the original material included in this paper. The authors also confirm that they have obtained permission, from the copyright holder of any third party material included in this paper, to publish